

Synthesis and Related Kinetics of Nanocrystalline Ni by Hydrogen Reduction of NiO

Jai-Sung Lee and Bum-Sung Kim

Department of Metallurgy and Materials Science, Hanyang University, Ansan 425-791, Korea

The present study has attempted to elucidate the formation mechanism of nanocrystalline (nc) Ni by hydrogen reduction of fine NiO powder in terms of related kinetics aspects. So, the kinetics and related mechanism of hydrogen reduction of NiO were investigated on the basis of structure modification of the NiO powder during reaction. The ball-milled NiO agglomerate powder having 20 nm in grain size and a log-normal pore size distribution was used for study. The non-isothermal reduction study showed that the nano-agglomerate NiO underwent a two-step reduction process which is presumably due to a chemical reaction at lower temperatures and a diffusion controlled process at higher temperatures. The activation energy for the nano-agglomerate NiO was 85.4 kJ/mol for lower temperatures and 105.1 kJ/mol for higher temperatures. The value for lower temperatures is consistent with that of as-received NiO of 85.6 kJ/mol. Such higher activation energy for higher temperatures can be attributed to the retardation of the reduction process by the change in the reduction mechanism from the chemical reaction to the diffusion process. Conclusively, the structure change during the reduction is believed to be responsible for the change in the reduction mechanism.

(Received March 1, 2001; Accepted May 8, 2001)

Keywords: powder synthesis, nanocrystalline nickel, hydrogen reduction, nickel oxide

1. Introduction

Recently, the issue of hydrogen reduction of ultra fine metal oxides has become desirable for the field of nanostructured materials synthesis for the applications of functional materials such as catalyst, magnetic-, optical- and electronic materials. This is because metal nano particulate materials with high purity can be produced by hydrogen reduction of fine metal oxides.¹⁻⁶⁾ In these nano-materials, the structure and properties of the nano-crystalline (nc) metal phase play a substantial role in determining the final properties and related applications.⁷⁻¹¹⁾

In recent years, it has been reported by the author's group that a distinct and unusual reduction behavior occurs during hydrogen reduction of ball-milled oxide powders of $\text{WO}_3\text{-CuO}^{5)}$ and $\text{NiO-Fe}_2\text{O}_3$.¹¹⁾ They found that the reaction during the hydrogen reduction proceeds in a two-step process while one continuous process takes place in the as-received oxides. This has an important implication in that such a discontinuous reduction process is closely related to the nano-porous structure of the ball-milled oxide agglomerates, resulting in a complexity of the reduction mechanism. Such a discontinuous type of hydrogen reduction process of NiO was observed earlier by Gallagher and his coworkers.¹²⁾ However, they did not explain the phenomenon and only tried to show that the magnetic properties or Ni had no influence on it. Other experimental evidence can be deduced from the previous works on reduction kinetics of NiO.^{13,14)} Sohn and Kim¹³⁾ experimentally found that the reduction of porous NiO powder by hydrogen gas is rate-controlled by a chemical reaction mechanism. Recently Sridhar *et al.*¹⁴⁾ also demonstrated that the reduction kinetics for NiO is controlled by a chemical reaction mechanism. However, they overlooked the significance of their nonlinear Arrhenius relationship of the reduction kinetics, implying the possibility of a mechanism change during the reduction process. In other words, the reduction kinetics in their work might not be controlled by a single mechanism.

This could be due to the fact that the structure and characteristics of NiO were not taken into account when considering the kinetics. Hence, the lack of unanimous kinetics for NiO hydrogen reduction, despite a number of previous studies can be attributed to the fact that there has not been an understanding of reduction behavior depending based on the structure of NiO.

From this point of view, it is important to understand exactly the reduction process of fine metal oxides in association with structure change. This is a prerequisite for optimization of the mechano-chemical process for synthesis of nano-materials from metal oxide. For this purpose, the present study attempted to investigate the synthesis and related kinetics of the reduction process depending on the structure of oxide agglomerates. As an experiment material, the NiO was selected for the study because it has only one stable phase, thus enabling it to ignore other complex reactions. Another reason why NiO was selected is because it has a great potential for utilization of catalyst as well as magnetic materials.¹⁵⁾ The reduction kinetics for nano-porous NiO agglomerate powder experiment was conducted by non-isothermal thermogravimetry (TG) and hygrometry studies, as well as isothermal kinetics study. Based on the results, the mechanism of hydrogen reduction of NiO was discussed in terms of the reaction kinetics.

2. Experimental Procedure

2.1 Materials

As a raw material for synthesis of nc Ni by hydrogen reduction, commercial NiO powder with a purity of 99.9% and a nominal average particle size of 7 μm was utilized. The powder was ball-milled for 10 h in a stainless steel attritor at a speed of 300 revolutions per minute. Methyl alcohol was used as a milling agent. After ball-milling the powder was dried at 333 K for 24 h. The dried cake that formed was crushed and sieved down to a mesh size of 20 μm . The aver-

age grain size was calculated by the Scherrer formula based on the X-ray diffraction method (XRD) using full width at half the maximum of the peak.¹⁶⁾ The pore size distributions and specific surface areas of NiO powders were measured by BET (Brunauer, Emmett and Teller) with the nitrogen adsorption method.¹⁷⁾

2.2 Kinetics study and microstructure characterization

The kinetics of reduction of the ball-milled NiO powders were measured by means of the measurement techniques of weight loss (TG) and water evaporation rate (hygrometry). These two measuring systems are equipped in one system so that one can conduct both measurements simultaneously. Namely, the gas outlet from TG system is directly connected with the humidity sensor of the hygrometry system, so that weight loss and water vapor removal can be measured simultaneously. It is noted here that the connecting tube passing the outlet gas from the TG system to the hygrometer was kept warm above room temperature to avoid condensation of water vapor below the dew point.

First, the TG setup comprised of a quartz reaction tube mounted vertically inside a tungsten lamp furnace. A small top-loading alumina crucible was used as a container mounted on an alumina pole extending from the microbalance. A shallow alumina crucible of a 5 mm inner diameter and 3 mm in height was used as the container to hold the oxide powder bed during the reaction. The powder bed was positioned in the uniform temperature zone of the furnace. Before heating, the furnace tube was evacuated and then flushed with argon gas. The powder sample was heated in a constant hydrogen gas flow (dew point 197 K) of 0.35 L/min at which any starvation of the reactant gas during the reduction could be avoided. The weight loss of the NiO powder was continuously monitored and the humidity level was checked every 10 s. The non-isothermal reduction studies were carried out at a temperature range from room temperature to 773 K with a heating rate of 10 K/min. For the isothermal reduction study, the ball-milled powders were reduced in the 550 to 623 K temperature range and the as-received powders were reduced in the 523 to 588 K temperature range. In these experiments, the temperature ranges were selected based on the results of TG and hygrometry studies.

In order to understand the reduction mechanism of NiO relating to powder structure, scanning electron microscopic (SEM) analyses of oxide and reduced samples were conducted. As well, pore size distribution of the powders was investigated using BET measurement. Kinetics and the related mechanism of hydrogen reduction of NiO were discussed, based upon the results of micro structure observation.

3. Results

3.1 Structure of ball-milled NiO powder

Figure 1 represents SEM morphologies of as-received NiO powder (a) in comparison with the ball-milled powder (b). It is seen that the ball-milled NiO powder in the agglomerate state is comprised of many nano-sized particles and pores less than 100 nm. Meanwhile, the as-received NiO shows dense surface structure with about 2 μm in grain size. XRD analysis of Fig. 2 reveals that the ball-milled NiO agglomerate shows

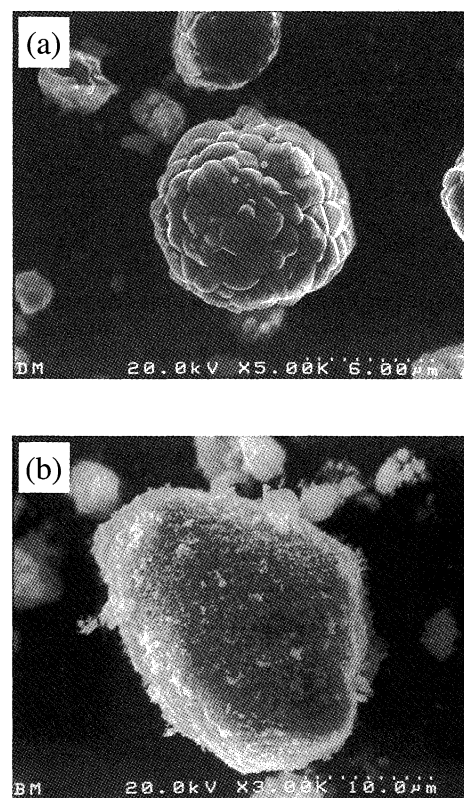


Fig. 1 SEM micrographs of (a) as-received and (b) ball-milled NiO powders.

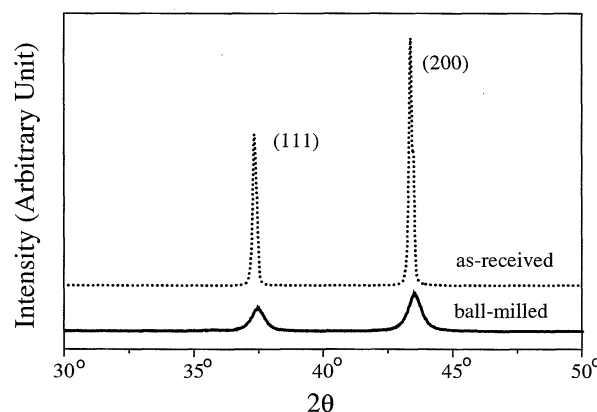


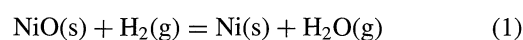
Fig. 2 XRD profiles of as-received and ball-milled NiO powders.

only the NiO phase and larger line broadening. The grain size of the ball-milled NiO powder calculated using Scherrer eq. based upon the XRD result amounts to 20–30 nm. This structural discrepancy between both NiO powders is reinforced by comparing the pore size distributions of Fig. 3. It demonstrates that the ball-milled oxide has a log-normal pore size distribution for intra-agglomerate pores having a size range below 100 nm. Contrary to this, as-received powder does not include nano-sized pores.

3.2 Reduction process of NiO powder

3.2.1 Non-isothermal behavior

The chemical reaction for the reduction process of NiO can be expressed as



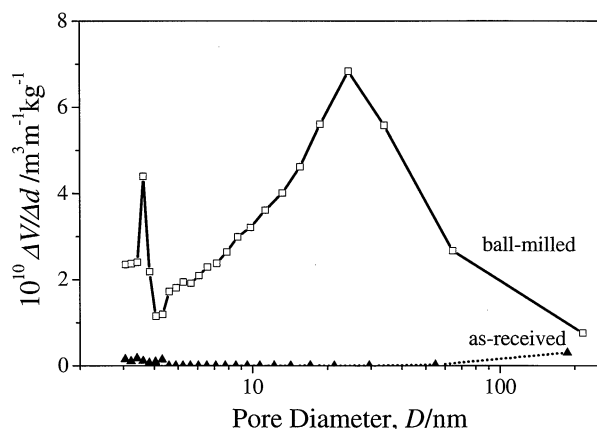


Fig. 3 Pore size distributions of as-received and ball-milled NiO powders.

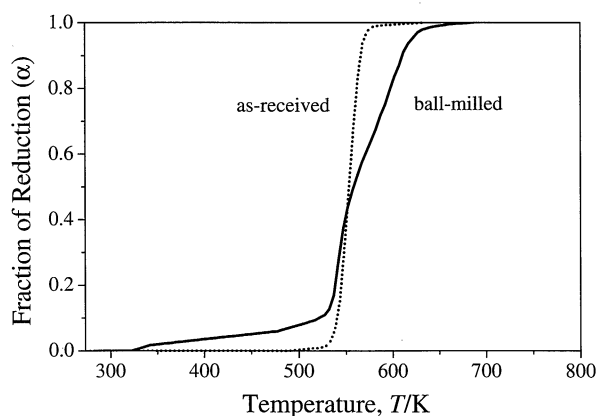


Fig. 4 TG curves for hydrogen reduction process of as-received and ball-milled NiO powders during heat-up to 773 K with the heating rate of 10 K/min.

Equation (1) shows that the hydrogen reduction of NiO produces a nickel phase leading to weight loss as a product of water vapor. Hence, the result of the TG study enables us to understand the reduction process for NiO. Figure 4 shows the TG curve for NiO powders in which nc NiO agglomerates undergo different weight loss behavior from the as-received oxide powder. Namely, the reduction started at a lower temperature but gradually retarded, and finally finished at a higher temperature when compared to the as-received oxide sample. Since the weight loss is due to removal of oxygen weight in the form of water vapor, the measurement of the water vapor generated during the reaction should give us very important information about the reaction mechanism.

Figure 5 shows the result of hygrometric measurement representing the removal rate of water vapor. While the as-received NiO powder shows a normal distribution for the removal rate of water vapor, this is not the case in the nc NiO agglomerate. In other words, the removal rate of water vapor in the nc oxide sample follows a stepwise process consisting of two peaks. Intuitively it seems that the reduction of NiO and the formation of Ni nano particles proceed in a different way in both cases. When we compare this result with the differential value of weight loss of Fig. 4, almost congruent behavior is observed in Fig. 6. This is strong evidence for the claim that the hydrogen reduction process of nc NiO powder follows the reaction of eq. (1) as described.

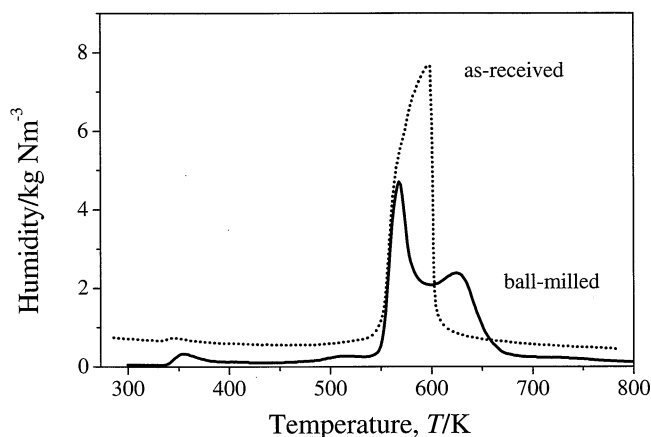


Fig. 5 Humidity curves for hydrogen reduction process of as-received and ball-milled NiO powders during heat-up to 773 K with the heating rate of 10 K/min.

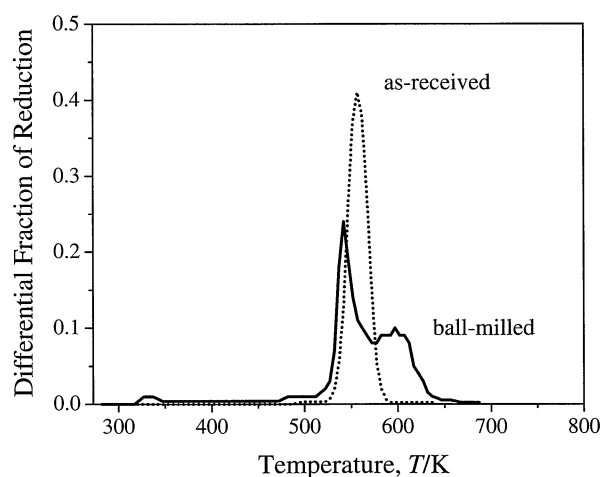


Fig. 6 Differential TG curves for hydrogen reduction process of as-received and ball-milled NiO powders during heat-up to 773 K with the heating rate of 10 K/min.

3.2.2 Isothermal behavior

In order to confirm the unusual differential TG behavior in nc NiO, we investigated the reaction kinetics with an isothermal kinetics experiment in the temperature ranges of two peaks of Fig. 5; 523–571 K for the as-received NiO and 513–623 K for the nc NiO agglomerate. The isothermal reduction curves measured in these temperature ranges are represented in Fig. 7. Here the fraction of reduction, α , is described by the ratio of the instant weight loss to the theoretical final weight loss. It is seen that the reaction rate consistently increases with the increase of temperature in both powder samples. However, a linear relationship for time dependence of the reduction fraction is observed differently in both cases. The as-received powder shows a linear reduction behavior for α up to 0.8, on the contrary, the ball-milled powder ceases to be linear at lower α values with decreasing temperature. Since there appears to be a change of reaction mechanism for α beyond this fraction, the reduction rate decreases dramatically. The value of α corresponding to this transition point decreases as the temperature increases. Beyond this point, a decrease of the reduction rate is observed with the increase of temperature.

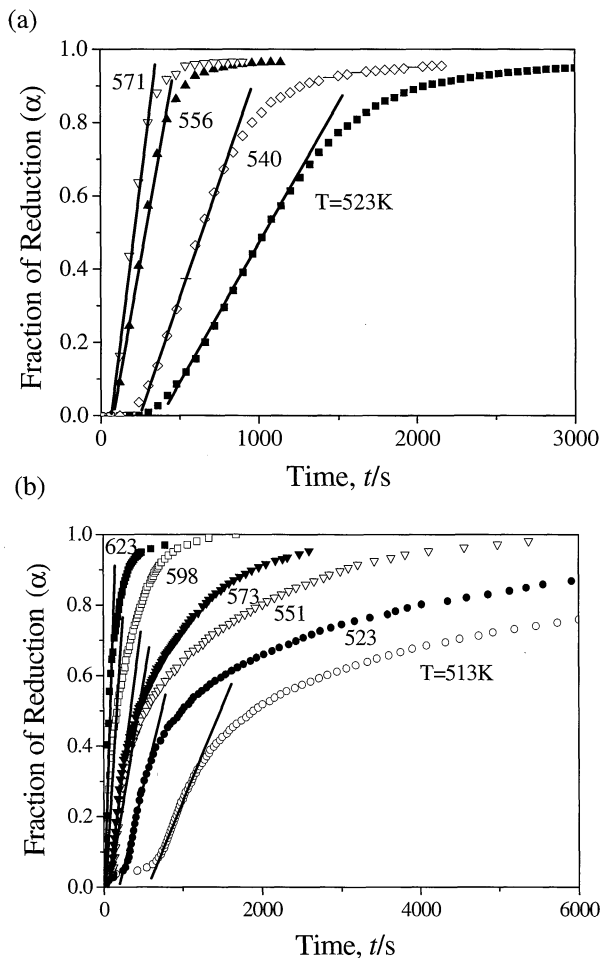


Fig. 7 Fraction of hydrogen reduction of (a) as-received and (b) ball-milled NiO powders versus time at various temperatures.

3.3 Microstructure of nc Ni powder

According to the TG curve in Fig. 4, the NiO samples were reduced during heat-up to 773 K in a hydrogen atmosphere at the heating rate of 10 K/min and quenched. Figure 8 discloses the morphologies of the reduced Ni powders. It is apparent that both powder samples keep the initial structure of oxide powders. Specially, the ball-milled agglomerate NiO powder is transformed to the Ni agglomerate, which is composed of ultra fine Ni particles. XRD analysis of Fig. 9 reveals that the line broadening of the ball-milled powder yielded the average grain size of 20 nm while the grain size of as-received sample could not be measured due to large grain size as depicted in Fig. 8.

4. Discussion

The most important result of the present investigation is that nc Ni phase of about 20 nm in grain size is successfully produced by hydrogen reduction of nano-agglomerate NiO depending on powder structure. In order to optimize the processing of nano-powder synthesis, it is essential to understand the reduction mechanism in kinetics aspect.

As described above, the ball-milled NiO agglomerate has a different powder structure from the as-received oxide powder. It was also described that the ball-milled oxide underwent an

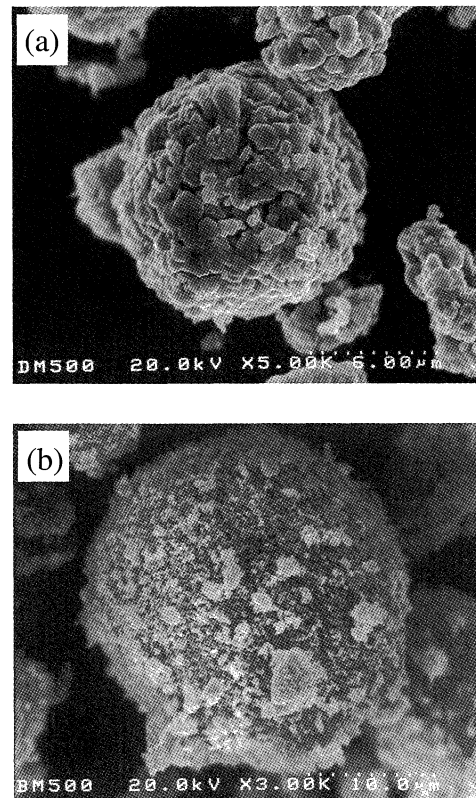


Fig. 8 SEM micrographs of Ni powders produced by hydrogen reduction of (a) as-received and (b) ball-milled NiO powders (heated-up to 773 K with the heating rate of 10 K/min and quenched).

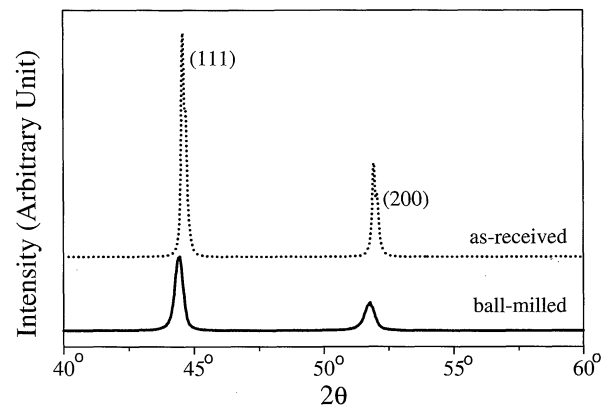


Fig. 9 XRD patterns of Ni powders represented in Fig. 8.

unusual reduction behavior during the reduction process as shown in TG and hygrometric studies.^{5,6} This structure related reduction process could be explained by estimating the reduction mechanism in terms of quantitative kinetics.

If the particles are assumed to be spherical, the "shrinkage-core model" can be applied to the individual particle. The relationship between the fraction of reaction, α , and time, t , has been derived for cases where either the chemical reaction or the diffusion through the product layer is the rate-controlling step. The relationship corresponding to reaction can be expressed as

$$t = \frac{\rho_{\text{NiO}} r_0}{M_{\text{NiO}} P_{\text{H}_2}} \frac{f(\alpha)}{k} \quad (2)$$

where ρ_{NiO} is the density, r_0 is the initial radius of the par-

ticle and M_{NiO} is the molecular weight of NiO, p_{H_2} is the partial pressure of hydrogen gas and k is the reaction rate constant.^{18–20} Since $\rho_{\text{NiO}}r_0/M_{\text{NiO}}p_{\text{H}_2}$ is constant at a given temperature, eq. (2) will lead to a linear relationship between $f(\alpha)$ and t . Equation (2) can be rearranged as

$$k = \frac{\rho_{\text{NiO}}r_0}{M_{\text{NiO}}p_{\text{H}_2}} \frac{f(\alpha)}{t} \quad (3)$$

The reaction rate constant k is a function of temperature and can be represented by the Arrhenius relationship

$$k = k_0 \exp\left(-\frac{Q}{RT}\right) \quad (4)$$

where k_0 is a constant, T is the temperature in K, R is the gas constant and Q represents the activation energy of the reduction reaction. Combining eqs. (3) and (4), the following relationship can be obtained.

$$\frac{f(\alpha)}{t} = \frac{M_{\text{NiO}}k_0p_{\text{H}_2}}{\rho_{\text{NiO}}r_0} \exp\left(-\frac{Q}{RT}\right) = k' \quad (5)$$

It is to be noticed that the left side of eq. (5) is equal to the value of the slope of the plot $f(\alpha)$ vs. t in Fig. 7. By taking the logarithm on both sides of eq. (5), we get the following relationship;

$$\ln(k') = \ln\left(\frac{f(\alpha)}{t}\right) = \ln\left(\frac{M_{\text{NiO}}k_0p_{\text{H}_2}}{\rho_{\text{NiO}}r_0}\right) - \left(\frac{Q}{R}\right)\left(\frac{1}{T}\right) \quad (6)$$

where the value of the slope corresponds to that of $f(\alpha)$ vs. t , which physically indicates the reaction rate constant. The slopes at various temperatures are obtained from the linear relationship presented in Fig. 7. When plotting the slopes in Arrhenius relationship of Fig. 10, the activation energy for the reduction process can be obtained. The as-received NiO powder reveals only one value of activation energy, 85.6 kJ/mol. Meanwhile, the ball-milled powder shows a discontinuous type of behavior in which the activation energy can be divided into two temperature regions; 85.4 kJ/mol below about 570 K and 105.1 kJ/mol above 570 K.

The most salient result of the activation energy is the observation that the fine agglomerate NiO undergoes a discontinuous reduction process. Such a discontinuity in the case of nano-agglomerate NiO implies a change of reduction mechanism depending on the temperature. The change of reduction mechanism has been already indicated by the results of the TG and hygrometry studies of Figs. 5 and 6. They clearly showed the occurrence of two independent reaction peaks with respect to the removal rate for hydrogen reduction of nano-agglomerate NiO. The first peak of a lower temperature range is sharp and narrow, which is similar in appearance to that of the as-received powder. On the other hand, the second peak of a higher temperature range, which overlapped with the first one, is much smaller and wider than the as-received NiO only. Moreover, the reaction due to this second peak finished at a much higher temperature than the as-received one.

Since the NiO powder bed in this study is very shallow (less than 1 mm in height), and the H_2 flow rate is reasonably high, the reactant gas, H_2 , has access to all the fine particles in the bed and the product gas, H_2O , can leave the site without any hindrance. For this reason, it is expected that

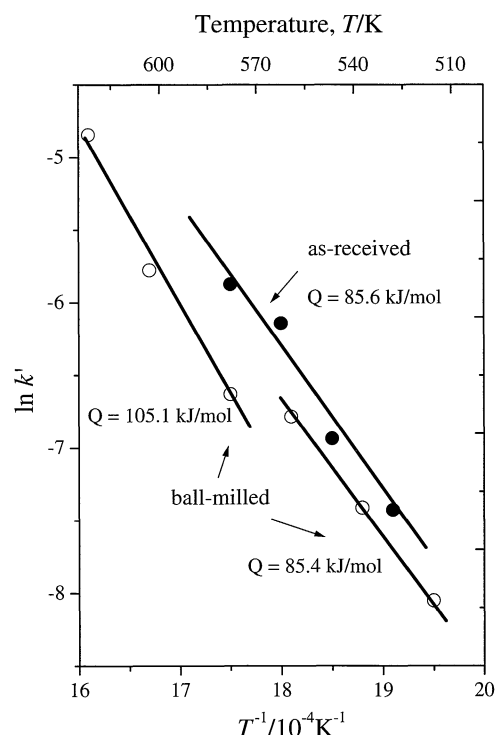


Fig. 10 Arrhenius plot for the isothermal hydrogen reduction rate of as-received and ball-milled NiO.

the reduction rate of the NiO powder used in this study is basically controlled by the chemical reaction before $\alpha = 0.8$ in Fig. 7(a). The decrease in the reduction rate beyond 0.8 could be due to the increase of the interdiffusion distance, consequently increasing the significance of the role of mass transfer in the rate-controlling process. As mentioned, the value of the fraction of reduction corresponding to the mechanism change decreased with increasing temperature. After this change, the reduction at a higher temperature had a somewhat lower reaction rate.¹⁴ This could be attributed to the concept that a denser product layer would be formed as the temperature is increased and hinders the reduction process. This argument seems reasonable considering the result of Fig. 7(b) in which the nano-agglomerate NiO powder shows different saturation temperatures. In view of this, the reduction of nano-agglomerate NiO powder is initially rate-controlled by the chemical reaction comprising a nucleation and growth mechanism which occurs rapidly representing a sharp and narrow peak of removal rate and growth. It then gradually proceeds by the diffusion controlled reaction showing a smaller and wider peak.

This interpretation is qualitatively consistent with the results of activation energy of Fig. 10. As can be seen in the result, the apparent activation energy, 85.4 kJ/mol for the nano-agglomerate oxide below 570 K is almost equal to that of the as received one, 85.6 kJ/mol. However, above 570 K the nano-agglomerate powder has a higher energy of 105.1 kJ/mol. The present data for apparent activation energy are comparable with the results of the previous works.^{21,22} Since the higher activation energy implies the retardation of the reduction process, the slow-down of the reaction in the case of the nano-agglomerate powder at higher temperatures

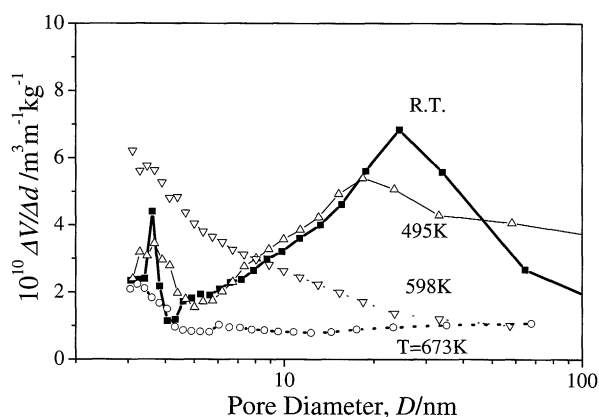


Fig. 11 Variation of pore size distribution during hydrogen reduction of ball-milled NiO agglomerate powder (heated-up with the heating rate of 10 K/min and quenched).

is presumably due to a slow-diffusion of removing water vapor through the dense product in the agglomerates. Regarding such a dramatic change of the reduction process in the ball-milled nano-agglomerate oxide powder, Lee and his coworkers^{6,23} suggested that structural modification of the agglomerate powder during reduction might be responsible for the mechanism change. Namely, in the initial stage of the reduction process, the reduction of the nano-agglomerate NiO occurs rapidly by a nucleation-growth mechanism. As the reaction proceeds, however, the reduced nano-sized Ni particles tend to be sintered together, leading to the decrease of nano-pore channel acting as a high diffusion path for removal of water vapor. It would be possible when the closure of intra-agglomerate pores hinder the further diffusion process for reaction. In other words, in the case of nano-agglomerate oxide, the reduction initially starts by the nucleation-growth process and then retards gradually due to the diffusion controlling process.

This explanation can be also reinforced in micro-structural aspects. As mentioned above, it became clear that the retardation of reduction kinetics of the nano-agglomerate NiO at higher temperatures is due to the decrease of pore channel for the gas diffusion path. This can be ascertained by the result of the pore size distribution changing during the reduction process. Figure 11 clearly discloses that with increasing temperature the distributions of nanosized pores smaller than 100 nm are gradually shifted to the much smaller range. This implies that the pore volume in the nano-agglomerates is decreased as the reduction proceeds.

5. Conclusions

In the present study the synthesis and related kinetics of nc Ni by hydrogen reduction of NiO were investigated by microstructure observation and reduction kinetics experiments using a TG and hygrometry. The ball-milled NiO agglomerate powder, which has 20 nm in grain size and a log-normal

pore size distribution in the range of below 100 nm, was used for this study. The non-isothermal reduction study showed that the nano-agglomerate NiO underwent a two-step reduction process, which is presumably due to a chemical reaction at lower temperatures and a diffusion controlled process at higher temperatures. The activation energy calculated from the isothermal kinetics study for the nano-agglomerate NiO was 85.4 kJ/mol for lower temperatures and 105.1 kJ/mol for higher temperatures. The value for lower temperatures is consistent with that of as-received NiO of 85.6 kJ/mol. Such higher activation energy for higher temperatures can be attributed to retardation of reduction process by the change of reduction mechanism from chemical reaction to the diffusion process. Conclusively, the structure change during reduction is believed to be responsible for the change of reduction mechanism.

Acknowledgements

This work is supported by the KOSEF and JPSP Joint Research Project under the Korea-Japan Basic Scientific Cooperation Program (Contact No. 976-0800-002-2).

REFERENCES

- 1) T. Sekino and K. Niihara: *NanoStr. Mater.* **6** (1995) 663–672.
- 2) J. Szekely and J. W. Evans: *Metall. Trans.* **2** (1971) 1699–1710.
- 3) J. W. Evans and S. Song: *Metall. Trans.* **4** (1973) 1701–1707.
- 4) Y. K. Rao: *Metall. Trans.* **10B** (1979) 243–255.
- 5) T. H. Kim, J. H. Yu and J. S. Lee: *NanoStr. Mater.* **9** (1997) 213–216.
- 6) J. S. Lee, T. H. Kim, J. H. Yu and S. W. Chung: *NanoStr. Mater.* **9** (1997) 153–156.
- 7) E. Breval, G. Dodds and C. G. Pantano: *Mater. Res. Bull.* **20** (1991) 1191–1205.
- 8) A. K. Khand and P. S. Nicholson: *J. Mater. Sci.* **15** (1980) 177–187.
- 9) P. Lou, T. G. Nieh, A. J. Schwartz and T. J. Lenk: *Mater. Sci. Eng.* **A204** (1995) 59–64.
- 10) X. Y. Qin, J. S. Lee and J. G. Kim: *J. Appl. Phys.* **86** (1999) 2146–2154.
- 11) X. Y. Qin, J. S. Lee, J. G. Nam and B. S. Kim: *NanoStr. Mater.* **11** (1999) 383–397.
- 12) P. K. Gallagher, E. M. Gyorgy and W. R. Jones: *J. Thermal Anal.* **23** (1982) 185–192.
- 13) H. Y. Sohn and D. S. Kim: *Metall. Trans.* **15B** (1984) 403–406.
- 14) S. Sridhar, D. Sichen and S. Seetharaman: *Z. Metallkd.* **85** (1994) 9–13.
- 15) X. L. Dong, Z. D. Shang, S. R. Jin, W. M. Sun and Y. C. Chuang: *NanoStr. Mater.* **10** (1997) 585–592.
- 16) B. D. Cullity: *Elements of X-Ray Diffraction*, 2nd Ed., (Addison-Wesley Publishing Company, INC., 1979) pp. 99–106.
- 17) R. M. German: *Powder Metallurgy Science*, 2nd Ed., (Metal Powder Industries Federation, New Jersey, 1994) pp. 69–70.
- 18) J. Szekely, J. W. Evans and H. Y. Sohn: *Gas Solid Reaction*, (Academic Press, INC. New York, 1976) pp. 65–104.
- 19) J. M. Smith: *Chemical Engineering Kinetics*, 3rd Ed., (McGraw-Hill Book Company, New York, 1981) pp. 763–770.
- 20) M. E. Brown: *Introduction to Thermal Analysis*, (Techniques and Applications, Chapman and Hall, 1988) pp. 127–151.
- 21) J. Bandrowski, C. R. Bickling, K. H. Yang and O. A. Houghen: *Chem. Eng. Sci.* **17** (1962) 379–390.
- 22) G. Parravano: *J. Am. Chem. Soc.* **74** (1952) 1194–1198.
- 23) B. S. Kim, J. S. Lee, T. Sekino, Y. H. Choa and K. Niihara: *Scripta Materialia*, (2001) in press.